Organometallics 1994, *13*, 2357-2364

Cluster Synthesis. 43. New Layer-Segregated Platinum–Ruthenium Cluster Complexes and Their Reactions with Diphenylacetylene

Richard D. Adams,* Thomas S. Barnard, Zhaoyang Li, Wengan Wu, and John Yamamoto

Department of Chemistry and Biochemistry, University of South Carolina, Columbia, South Carolina 29208

Received February 16, 1994[⊗]

The new complex $Pt_3Ru_6(CO)_{21}(\mu\text{-}H)_3(\mu_3\text{-}H)$ (1) was obtained in 83% yield from the reaction of $Ru_4Pt_2(CO)_{18}$ with hydrogen (1 atm) at 97 °C. The molecular structure was found to consist of three triangular layers of nine metal atoms arranged in the form of a face-shared bioctahedron. The central shared layer consists of three platinum atoms, while the outer layers consist of ruthenium triangles. Three hydride ligands bridge each edge of one Ru_3 triangle, while the fourth hydride ligand is a triple bridge across the other Ru_3 triangle. Compound 1 was converted to the alkyne complex $Pt_3Ru_6(CO)_{20}(\mu_3\text{-}PhC_2Ph)(\mu_3\text{-}H)(\mu\text{-}H)$ (2) by reaction with PhC_2Ph. This complex contains a layered structure of Pt_3 and Ru_3 triangles similar to 1 but also has a triply bridging PhC_2Ph ligand coordinated to one of the ruthenium triangles. Compound 2 slowly adds 1 equiv of CO to form the complex $Pt_3Ru_6(CO)_{21}[\mu\text{-}PhCC(H)Ph](\mu\text{-}H)$ (3) which contains an edge bridging σ–π coordinated diphenylvinyl ligand formed by the transfer of one of the hydride ligands in 2 to the diphenylacetylene ligand. Treatment of 3 with CO yields (*Z*)-stilbene by transfer of the remaining hydride ligand to the diphenylvinyl ligand, and the cluster is then degraded to $Ru_3(CO)_{12}$ and $Pt_2Ru_4(CO)_{18}$. Crystal Data: for 1, space group = $P2_1/c$, a = 18.157(3) Å, b = 11.701(4) Å, c = 17.580(4) Å, β = 101.03(2)°, Z = 4, 2657 reflections, R = 0.033; for 2, space group $Pccn$, a = 10.848(2) Å, b = 45.507(4) Å, c = 17.169(2) Å, Z = 8, 4441 reflections, R = 0.043; for 3, space group $P2_1/c$, a = 12.360(6) Å, b = 11.521(4) Å, c = 16.628(8) Å, β = 106.10(4)°, Z = 2, 2061 reflections, R = 0.041.

Introduction

Certain metal alloy catalysts have been shown to exhibit unique reactivity that may be attributed to preferential interactions of the substrates at the sites of the different types of metals.[1] Recent studies have indicated that some metal cluster complexes are capable of performing a variety of organic reactions catalytically,[2] and there is evidence that some mixed-metal complexes may exhibit reactivity changes due to cooperative interactions between the different types of metal atoms.[3]

Our recent research has focused on the synthesis and reactivity of mixed-metal cluster complexes containing platinum and one of the elements iron,[4] ruthenium,[5] or osmium.[6] In high-nuclearity species we have observed a high tendency of the metal atoms to segregate their metal atoms into layers of the pure elements. We have now prepared the new layer-segregated metal cluster complex $Pt_3Ru_6(CO)_{21}(\mu\text{-}H)_3(\mu_3\text{-}H)$ (1) by the reaction of $Ru_4Pt_2(CO)_{18}$ with hydrogen. Compound 1 reacts selectively with PhC_2Ph to yield the alkyne complex $Pt_3Ru_6(CO)_{20}(\mu_3\text{-}PhC_2Ph)(\mu_3\text{-}H)(\mu\text{-}H)$ (2), in which the alkyne ligand is coordinated to one of the ruthenium triangles. The hydride ligands in 2 can be sequentially transferred to the PhC_2Ph ligand to form (*Z*)-stilbene by a series of CO addition reactions to 2. Compound 2 has recently been reported to be an effective catalyst for the hydrogenation of PhC_2Ph to (*Z*)-stilbene, Ph(H)C=C(H)Ph.[7]

Experimental Section

Reactions were performed under an atmosphere of dry nitrogen. Reagent grade solvents were dried over molecular sieves and deoxygenated by purging with nitrogen prior to use. IR spectra were recorded on a Nicolet 5DXB FT-IR spectrophotometer. A Bruker AM-300 FT-NMR spectrometer was used to obtain ^1H NMR spectra. Elemental microanalyses were performed by Desert Analytics, Tucson, AZ. TLC separations were performed by using silica gel (60 Å, F_{254}) on plates (Whatman

---

[⊗] Abstract published in *Advance ACS Abstracts*, May 1, 1994.

[1] (a) Sinfelt, J. H. *Bimetallic Catalysts. Discoveries, Concepts and Applications*; Wiley: New York, 1983. (b) Sinfelt, J. H. *Sci. Am.* **1985**, *253*, 90. (c) Sinfelt, J. H. *Acc. Chem. Res.* 1977, *10*, 15. (d) Sachtler, W. M. H. *J. Mol. Catal.* **1984**, *25*, 1. (e) Ponec, V. *Adv. Catal.* **1983**, *32*, 149. (f) Biswas, J.; Bickle, G. M.; Gray, P. G.; Do, D. D.; Barbier, J. *Catal. Rev.—Sci. Eng.* **1988**, *30*, 161. (g) Goodman, D. W.; Houston, J. E. *Science* **1987**, *236*, 403.

[2] (a) Süss-Fink, G.; Meister, G. *Adv. Organomet. Chem.* **1993**, *35*, 41. (b) Süss-Fink, G.; Neumann, F. *The Chemistry of the Metal-Carbon Bond*; Hartley, F. R., Ed.; Wiley: Chichester, England, 1989; Vol. 5, p 231. (c) Gates, B. C., Guczi, L., Knözinger, H., Eds. *Metal Clusters in Catalysis*; Elsevier: Amsterdam, The Netherlands, 1986. (d) Gladfelter, W.; Roesselet, K. J. *The Chemistry of Metal Cluster Complexes*; Shriver, D., Kaesz, H. D., Adams, R. D., Eds.; VCH: Weinheim, Germany, 1990; Chapter 7, p 329. (e) Castiglioni, M.; Giordano, R.; Sappa, E. *J. Organomet. Chem.* **1989**, *369*, 419.

[3] (a) Braunstein, P.; Rosé, J. In *Stereochemistry of Organometallic and Inorganic Compounds*; Bernal, I., Ed.; Elsevier: Amsterdam, 1989; Vol. 3. (b) Giordano, R.; Sappa, E. *J. Organomet. Chem.* **1993**, *448*, 157.

[4] Adams, R. D.; Arafa, I.; Chen, G.; Lii, J. C.; Wang, J. G. *Organometallics* **1990**, *9*, 2350.

[5] (a) Adams, R. D.; Li, Z.; Lii, J. C.; Wu, W. *Organometallics* **1992**, *11*, 4001. (b) Adams, R. D.; Li, Z.; Lii, J. C.; Wu, W. *Inorg. Chem.* **1992**, *31*, 3445. (c) Adams, R. D.; Chen, G.; Wu, W. *J. Cluster Sci.* **1993**, *4*, 119. (d) Adams, R. D.; Alexander, M. S.; Arafa, I.; Wu, W. *Inorg. Chem.* **1991**, *30*, 4717.

[6] (a) Adams, R. D.; Lii, J. C.; Wu, W. *Inorg. Chem.* **1992**, *31*, 2556. (b) Adams, R. D.; Lii, J. C.; Wu, W. *Inorg. Chem.* **1991**, *30*, 2257. (c) Adams, R. D.; Lii, J. C.; Wu, W. *Inorg. Chem.* **1991**, *30*, 3613. (d) Adams, R. D.; Chen, G.; Lii, J. C.; Wu, W. *Inorg. Chem.* **1991**, *30*, 1007. (e) Adams, R. D.; Wu, W. *Inorg. Chem.* **1991**, *30*, 3605.

[7] Adams, R. D.; Li, Z.; Wu, W.; Swepston, P.; Yamamoto, J. *J. Am. Chem. Soc.* **1992**, *114*, 10657.

0276-7333/94/2313-2357$04.50/0

Table 1. Crystal Data for Compounds 1–3

	1	2	3
empirical formula	$Pt_3Ru_6O_{21}C_{21}H_4 \cdot 0.5CH_2Cl_2$	$Pt_3Ru_6O_{20}C_{34}H_{12}$	$Pt_3Ru_6O_{21}C_{35}H_{12}$
fw	1826.4	1932.15	1960.16
cryst syst	monoclinic	orthorhombic	monoclinic
lattice params			
a (Å)	18.157(3)	10.848(2)	12.360(6)
b (Å)	11.701(4)	45.507(4)	11.521(4)
c (Å)	17.580(4)	17.169(2)	16.628(8)
β (deg)	101.03(2)	90.00	106.10(4)
V (Å³)	3666(3)	8480(1)	2275(2)
space group	$P2_1/c$ (No. 14)	*Pccn* (No. 56)	$P2_1$ (No. 4)
Z	4	8	2
ρ_{calc} (g/cm³)	3.31	3.03	2.86
$\mu(K\alpha)$ (cm^{-1})	140.3 (Mo)	361.7 (Cu)	112.6 (Mo)
temp (°C)	20	20	20
$2\theta_{max}$ (deg)	40.0	120.0	45.
no. of observns ($I > 3\sigma(I)$)	2657	4441	2061
no. of variables	380	553	412
residuals: R, R_w	0.033, 0.035	0.043, 0.051	0.041, 0.038
goodness of fit	1.76	2.16	1.28
largest peak in final diff map, (e/Å³)	1.12	2.61	1.08
abs cor	empirical	empirical	empirical

0.25-mm thickness). $Pt_2Ru_4(CO)_{18}$[5c] and $[Ru_3O(O_2CCH_3)_6(H_2O)_3]O_2CCH_3$[8] were prepared by previously reported procedures.

Preparation of $Pt_3Ru_6(CO)_{21}(\mu\text{-}H)_3(\mu_3\text{-}H)$ (1). A 25.0-mg amount of $Ru_4Pt_2(CO)_{18}$ dissolved in 140 mL of heptane was heated to reflux for 15 min in the presence of a slow purge with hydrogen. A small amount of dark precipitate formed and was removed by filtration. The solvent was removed from the filtrate, and the residue was washed with pentane several times to yield pure 1 (16.1 mg). An additional 3.0 mg of 1 was subsequently obtained from the washings by TLC using hexane/CH_2Cl_2 (3/1) solvent. Total yield: 19.1 mg (83%). IR for 1 (ν(CO), cm^{-1}; in CH_2Cl_2): 2081 (w, sh), 2066 (vs), 2052 (m, sh), 2026 (w). ^1H NMR (δ; in acetone at −88 °C): −15.84 (s, 3H), −19.26 (s, 1H). ^{13}C NMR (δ; in CD_2Cl_2 at 25 °C): 189.77 (s, CO). Anal. Calcd (found): C, 14.14 (14.49); H, 0.23 (0.26).

Preparation of $Pt_3Ru_6(CO)_{20}(\mu_3\text{-}PhC_2Ph)(\mu_3\text{-}H)(\mu\text{-}H)$ (2). A 20.0-mg amount (0.0112 mmol) of 1 and 5.0 mg (0.0281 mmol) of PhC_2Ph was dissolved in 150 mL of hexane, and the solution was refluxed for 60 min. Separation by TLC using hexane/CH_2Cl_2 (3/1) solvent yielded gray-green $Ru_7Pt_3(CO)_{22}(\mu_3\text{-}H)_2$[2d] (1.2 mg), followed by gray-brown 2 (5.4 mg, 25%) and green-brown $Pt_3Ru_6(CO)_{14}(\mu_3\text{-}PhC_2Ph)_3$[10] (1.3 mg, 6%). IR for 2 (ν(CO), cm^{-1}; in CH_2Cl_2): 2098 (w), 2065 (vs), 2033 (m), 2015 (w, sh), 2000 (w, sh), 1950 (vw, sh). ^1H NMR (δ; in CD_2Cl_2 at −58 °C): 7.70–7.05 (m, 10H), −17.97 (s, 1H), −18.71 (s, 1H). Anal. Calcd (found): C, 21.14 (20.67); H, 0.63 (0.72). In addition, the reaction of 5.0 mg of 1 with 0.7 mg of PhC_2Ph (1:1.3) was performed in 10 mL of benzene-d_6 solvent by heating to reflux for 1 h. An NMR spectrum of the entire reaction mixture was recorded after concentrating the solution to 1 mL. This spectrum showed a strong signal at 6.48 ppm that is attributed to (*Z*)-stilbene.[9]

Preparation of $Pt_3Ru_6(^{13}CO)_{21}(\mu\text{-}H)_3(\mu_3\text{-}H)$ (1*) and $Pt_3Ru_6(^{13}CO)_{20}(\mu_3\text{-}PhC_2Ph)(\mu_3\text{-}H)(\mu\text{-}H)$ (2*). $[Ru_3O(O_2CCH_3)_6(H_2O)_3]O_2CCH_3$ (500 mg, 0.636 mmol) was allowed to react with ^{13}CO (99% ^{13}C enriched) to form $Ru_3(^{13}CO)_{12}$ (198 mg).[11] This $Ru_3(^{13}CO)_{12}$ was dissolved in 500 mL of hexane in a 1000-mL three necked flask and was converted to $Ru(^{13}CO)_5$ by photolysis in the presence of 1 atm of ^{13}CO. Without isolation, $Pt(COD)_2$ (198 mg, 0.482 mmol) was added to the solution of $Ru(^{13}CO)_5$ at 0 °C to yield $Ru_4Pt_2(^{13}CO)_{18}$ (138 mg). $Ru_4Pt_2(^{13}CO)_{18}$ was converted to 1* and then 2* by the procedures described above. The ^{13}C NMR sample of 2* was prepared with 10 mg of the complex dissolved in 0.6 mL of CD_2Cl_2. ^{13}C NMR (δ; in $CDCl_3$ at 25 °C): 201.93 (s, 2CO), 197.02 (d, 2CO, $^3J_{^{13}C-^{13}C}$ = 11.1 Hz), 195.5 (s, 2CO), 194.69 (d, 1CO, $^3J_{^{13}C-^{13}C}$ = 11.1 Hz), 192.43 (s, 6CO), 190.34 (s, 4CO), 190.00 (s, 3CO). ^{13}C NMR (δ; in CD_2Cl_2 at −85 °C): 202.3 (s, 2CO), 197.7 (d, 2CO, $^3J_{^{13}C-^{13}C}$ = 11 Hz), 195.9 (s, 2CO), 195.0 (d, 1CO, $^3J_{^{13}C-^{13}C}$ = 11 Hz), 192.3 (s, 6CO), 190.8 (s, 2CO), 190.4 (s, 2CO), 190.1 (s, 3CO).

Reaction of 2 with PhC_2Ph. A 9.0-mg amount (0.006 46 mmol) of 2 and an 11.7-mg amount (0.0657 mmol) of PhC_2Ph were dissolved in 35 mL of hexane, and the solution was heated to reflux for 4 h. After the solvent was removed, the residue was worked up by TLC (hexane/CH_2Cl_2 = 3/1), affording 1.9 mg of unreacted 2 and 5.7 mg of $Ru_6Pt_3(CO)_{14}(\mu_3\text{-}PhC_2Ph)_3$ (58%).

Reaction of 2 with CO. A 10.0-mg amount of 2 (0.005 18 mmol) was dissolved in a solvent mixture of 6 mL of CH_2Cl_2 and 30 mL of hexane in a three-necked 50-mL flask. The solution was slowly purged with CO at 25 °C/1 atm for 4 h. The solvent was removed, and the residue was separated by TLC using a hexane/CH_2Cl_2 (3/2) solvent mixture to yield, in the order of elution, 0.5 mg of $Ru_3(CO)_{12}$ (7%), 0.5 mg of $Ru_4Pt_2(CO)_{18}$ (5%), 5.0 mg of unreacted 2, and 1.1 mg of $Pt_3Ru_6(CO)_{21}[\mu\text{-}PhCC(H)Ph](\mu\text{-}H)$ (3; 11%). IR for 3: (ν(CO), cm^{-1}; in hexane): 2096 (w), 2069 (vs), 2058 (vs), 2042 (s), 2034 (w, sh), 1980 (vw), 1893 (vw), 1855 (w). ^1H NMR (δ; in $CDCl_3$ at 25 °C) 7.70–7.05 (m, 10H), 5.26 (s, 1H), −22.77 (s, 1H). Anal. Calcd (found): C, 21.44 (22.37); H, 0.62 (0.94).

Reaction of 3 with CO. A 5.1-mg amount of 3 (0.0026 mmol) was dissolved in 25 mL of hexane in a three-necked 50-mL round-bottom flask. This solution was purged slowly with CO at 25 °C for 2 days and then heated to reflux for 3 h. After the mixture was cooled, the solvent was removed under vacuum, and the residue was separated by TLC using hexane solvent to yield 0.40 mg of (*Z*)-stilbene (85%), 2.80 mg of $Ru_3(CO)_{12}$, and 0.50 mg of $Ru_4Pt_2(CO)_{18}$.

Crystallographic Analyses. Crystals of 1–3 were obtained by slow evaporation of solvent at 25 °C from solutions in hexane/CH_2Cl_2 solvent mixtures. The crystals used in the data collections were mounted in thin-walled glass capillaries. Diffraction measurements on compounds 1 and 3 were made on a Rigaku AFC6S automatic diffractometer by using graphite-monochromated Mo Kα radiation. Diffraction measurements on compound 2 were made on a Rigaku AFC5R rotating anode automatic diffractometer by using graphite-monochromated Cu Kα radiation. The unit cells were determined and refined from 25 randomly selected reflections obtained by using the automatic search, center, index, and least-squares routines. Crystal data, data collection parameters, and results of the analyses are listed in Table 1. All data processing was performed on a Digital Equipment Corp. VAXstation 3520 computer by using the TEXSAN structure solving program library (version 2.0) obtained from Molecular Structure Corp., The Woodlands, TX. Neutral atom scattering factors were obtained from the standard source.[12a] Anomalous dispersion corrections were applied to all non-hydrogen atoms.[12b] For all analyses the positions of the metal atoms were determined by direct methods (MITHRIL), and all other non-hydrogen atomic positions were obtained from subsequent difference Fourier syntheses.

Compound 1 crystallized in the monoclinic crystal system. The space group $P2_1/c$ was established from systematic absences observed in the data. The structure was solved by a combination of direct methods (MITHRIL) and difference Fourier techniques. All atoms heavier than carbon were refined with anisotropic thermal parameters. The hydride ligands were located and refined on their coordinates only. The crystal also contained 0.5 equiv of CH_2Cl_2 from the crystallization solvent. This was included in the analysis and satisfactorily refined.

---

[8] (a) Spencer, A.; Wilkinson, G. *J. Chem. Soc., Dalton Trans.* **1972**, 1570. (b) Louda, S. A.; Rempel, G. L. *Inorg. Chem.* **1979**, *18*, 1.

[9] Pouchert, C. J. *Aldrich Library of NMR Spectra*, 2nd ed.; Aldrich: Milwaukee, WI, 1983; Vol. 1, p 1752.

[10] Adams, R. D.; Wu, W. *Organometallics* **1992**, *12*, 1248.

[11] James, B. R.; Rempel, G. L.; Teo, W. K. *Inorg. Synth.* **1976**, *16*, 45.

[12] (a) *International Tables for X-ray Crystallography*; Kynoch Press: Birmingham, England, 1975; Vol. IV, Table 2.2B, pp 99–101. (b) *Ibid.*, Table 2.3.1, pp 149–150.

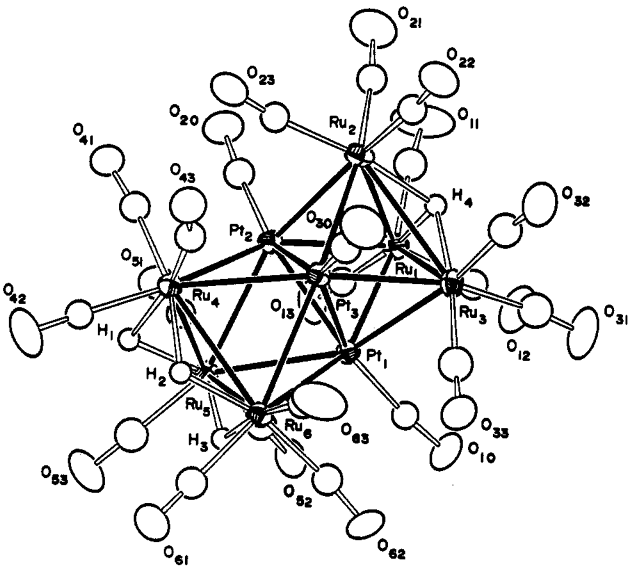

Figure 1. ORTEP diagram of $Pt_3Ru_6(CO)_{21}(\mu\text{-}H)_3(\mu_3\text{-}H)$ (1) showing 35% probability thermal ellipsoids for the non-hydrogen atoms.

Compound 2 crystallized in the orthorhombic crystal system. The space group *Pccn* was established from the systematic absences observed in the data. Due to the presence of one very long lattice parameter, $b = 45.509(2)$ Å, it was not possible to obtain a good-quality analysis using molybdenum radiation; therefore, the data for compound 2 were collected using copper $K\alpha$ radiation at the Molecular Structure Corp., The Woodlands, TX. All non-hydrogen atoms were refined with anisotropic thermal parameters. The positions of the hydride ligands were obtained from a difference Fourier map, but these positions were not refined. Hydrogen atom positions on the PhC_2Ph ligand were calculated and were included in the structure factor calculations, but they were not refined.

Compound 3 crystallized in the monoclinic crystal system. The pattern of systematic absences observed in the data were consistent with either of the space groups $P2_1$ and $P2_1/m$. It was not possible to obtain a suitable solution in the space group $P2_1/m$, but a good solution was obtained in the space group $P2_1$. The structure was solved by a combination of direct methods (MITHRIL) and difference Fourier techniques. Due to the limited number of data, only the atoms heavier than carbon were refined with anisotropic thermal parameters. The hydride ligand was located and refined on its positional parameters only. All other hydrogen atom positions were calculated and were included in the structure factor calculations but were not refined. To test for the enantiomorph, the coordinates of all of the atoms were inverted and the complete structure was refined again. For this enantiomorph, the final residuals were $R = 0.045$ and $R_w = 0.045$, which are significantly higher than those of the first enantiomorph; thus, the first enantiomorph was deemed to be correct and the results of the latter refinement were discarded.

Table 2. Positional Parameters and B(eq) Values for $Pt_3Ru_6(CO)_2(\mu\text{-}H)_4$ (1)[a]

atom	x	y	z	B(eq), Å^2
Pt(1)	0.70590(04)	0.08518(06)	0.28554(04)	2.28(3)
Pt(2)	0.78464(04)	0.09540(06)	0.17482(04)	2.24(3)
Pt(3)	0.79490(04)	−0.08588(06)	0.26619(04)	2.25(3)
Ru(1)	0.63247(10)	0.08798(14)	0.13618(09)	2.98(7)
Ru(2)	0.73761(10)	−0.11079(12)	0.11325(09)	2.87(8)
Ru(3)	0.64442(10)	−0.12149(13)	0.24045(09)	2.97(8)
Ru(4)	0.92529(09)	0.06083(12)	0.27853(08)	2.41(7)
Ru(5)	0.82395(09)	0.25569(12)	0.30083(08)	2.38(7)
Ru(6)	0.83512(09)	0.04865(12)	0.40623(08)	2.55(7)
O(10)	0.5675(09)	0.1625(13)	0.3440(09)	5.9(9)
O(11)	0.5748(12)	0.1020(16)	−0.0376(09)	10(1)
O(12)	0.4717(10)	0.1256(15)	0.1550(11)	7(1)
O(13)	0.6509(08)	0.3439(12)	0.1416(09)	5.0(8)
O(20)	0.8000(10)	0.1775(13)	0.0179(08)	5.7(9)
O(21)	0.6928(10)	−0.0793(13)	−0.0603(08)	7(1)
O(22)	0.8957(10)	−0.1283(12)	0.0883(09)	5.7(9)
O(23)	0.7256(10)	−0.3666(11)	0.0922(09)	5.8(9)
O(30)	0.8263(10)	−0.3374(12)	0.2877(09)	6.3(9)
O(31)	0.4789(10)	−0.1007(16)	0.2453(11)	8(1)
O(32)	0.6212(10)	−0.3740(13)	0.2088(10)	7(1)
O(33)	0.6703(09)	−0.1691(13)	0.4123(08)	6.0(9)
O(41)	0.9656(09)	0.1232(11)	0.1236(08)	4.8(8)
O(42)	1.0835(09)	0.1211(12)	0.3643(09)	6.1(8)
O(43)	0.9789(08)	−0.1840(11)	0.2660(08)	4.9(8)
O(51)	0.8262(09)	0.3929(11)	0.1564(08)	5.0(8)
O(52)	0.6840(8)	0.3806(11)	0.3300(09)	5.3(8)
O(53)	0.9206(11)	0.4340(14)	0.3995(10)	8(1)
O(61)	0.9516(09)	0.1234(12)	0.5464(08)	5.3(8)
O(62)	0.7049(09)	0.0869(13)	0.4887(07)	5.0(8)
O(63)	0.8494(11)	−0.1988(12)	0.4584(08)	7(1)
C(10)	0.6239(13)	0.1367(15)	0.3238(11)	3.0(4)
C(11)	0.6006(13)	0.0917(18)	0.0262(13)	4.6(5)
C(12)	0.5318(13)	0.1059(17)	0.1480(11)	3.7(5)
C(13)	0.6455(12)	0.2477(18)	0.1407(11)	3.4(4)
C(20)	0.7953(12)	0.1508(17)	0.0801(13)	3.8(5)
C(21)	0.7051(12)	−0.0903(17)	0.0067(12)	3.6(4)
C(22)	0.8389(13)	−0.1158(17)	0.1000(11)	3.3(5)
C(23)	0.7261(11)	−0.2706(18)	0.1003(11)	3.3(4)
C(30)	0.8151(12)	−0.2419(19)	0.2818(11)	3.9(5)
C(31)	0.5379(15)	−0.1065(19)	0.2373(13)	4.8(5)
C(32)	0.6303(13)	−0.2779(20)	0.2160(12)	4.5(5)
C(33)	0.6606(14)	−0.1489(19)	0.3477(14)	4.8(5)
C(41)	0.9452(12)	0.0997(17)	0.1799(12)	3.6(5)
C(42)	1.0244(12)	0.1005(16)	0.3309(11)	3.1(4)
C(43)	0.9488(12)	−0.0942(18)	0.2692(11)	3.7(4)
C(51)	0.8202(12)	0.3355(17)	0.2073(12)	3.5(4)
C(52)	0.7352(13)	0.3297(18)	0.3176(11)	3.8(5)
C(53)	0.8837(14)	0.3676(19)	0.3629(13)	4.7(5)
C(61)	0.9084(13)	0.0980(17)	0.4945(12)	3.8(5)
C(62)	0.7515(13)	0.0724(17)	0.4527(12)	3.8(5)
C(63)	0.8381(12)	−0.1114(18)	0.4341(12)	3.9(5)

[a] Estimated standard deviations in this and all following tables are given in parentheses.

Table 3. Intramolecular Distances (Å) for 1

Pt(1)–Pt(2)	2.629(1)	Ru(1)–H(4)	2.0(1)
Pt(1)–Pt(3)	2.635(1)	Ru(2)–Ru(3)	3.054(3)
Pt(1)–Ru(1)	2.708(2)	Ru(2)–H(4)	1.9(2)
Pt(1)–Ru(3)	2.717(2)	Ru(3)–H(4)	1.9(1)
Pt(1)–Ru(5)	2.903(2)	Ru(4)–Ru(5)	3.002(2)
Pt(1)–Ru(6)	2.878(2)	Ru(4)–Ru(6)	3.024(2)
Pt(2)–Pt(3)	2.646(1)	Ru(4)–H(1)	1.9(1)
Pt(2)–Ru(1)	2.717(2)	Ru(4)–H(2)	1.9(1)
Pt(2)–Ru(2)	2.715(2)	Ru(5)–Ru(6)	3.033(2)
Pt(2)–Ru(4)	2.869(2)	Ru(5)–H(1)	1.9(2)
Pt(2)–Ru(5)	2.886(2)	Ru(5)–H(3)	1.6(1)
Pt(3)–Ru(2)	2.707(2)	Ru(6)–H(2)	1.8(2)
Pt(3)–Ru(3)	2.715(2)	Ru(6)–H(3)	2.0(1)
Pt(3)–Ru(4)	2.899(2)	Pt–C (av)	1.85(2)
Pt(3)–Ru(6)	2.896(2)	Ru–C (av)	1.89(2)
Ru(1)–Ru(2)	3.084(2)	O–C (av)	1.14(3)
Ru(1)–Ru(3)	3.043(2)		

Results

The new complex $Pt_3Ru_6(CO)_{21}(\mu\text{-}H)_3(\mu_3\text{-}H)$ (1) was obtained in 83% yield from the reaction of $Ru_4Pt_2(CO)_{18}$ with hydrogen (1 atm) in a refluxing solution in heptane solvent (97 °C). Compound 1 was characterized by a single-crystal X-ray diffraction analysis, and an ORTEP diagram of its molecular structure is shown in Figure 1. Final atomic positional parameters for 1 are listed in Table 2. Selected bond distances and angles are given in Tables 3 and 4, respectively. The structure consists of three triangular layers of nine metal atoms arranged in the form of a face-shared bioctahedron. The central layer consists of three platinum atoms, while the outer layers are pure ruthenium. There is a hydride ligand bridging each edge of the Ru-

Table 4. Intramolecular Bond Angles (deg) for 1

Pt(2)–Pt(1)–Ru(3)	94.34(5)	Pt(2)–Pt(3)–Ru(6)	93.29(5)
Pt(2)–Pt(1)–Ru(6)	94.05(5)	Ru(2)–Pt(3)–Ru(4)	106.94(5)
Pt(3)–Pt(1)–Ru(1)	94.84(5)	Ru(2)–Pt(3)–Ru(6)	152.83(5)
Pt(3)–Pt(1)–Ru(5)	94.24(5)	Ru(3)–Pt(3)–Ru(4)	152.24(5)
Ru(1)–Pt(1)–Ru(5)	107.41(5)	Ru(3)–Pt(3)–Ru(6)	107.89(6)
Ru(1)–Pt(1)–Ru(6)	153.80(6)	Pt(1)–Ru(1)–Ru(2)	85.15(5)
Ru(3)–Pt(1)–Ru(5)	153.32(6)	Pt(2)–Ru(1)–Ru(3)	85.60(6)
Ru(3)–Pt(1)–Ru(6)	108.32(5)	Pt(2)–Ru(2)–Ru(3)	85.44(5)
Pt(1)–Pt(2)–Ru(2)	94.63(5)	Pt(1)–Ru(3)–Ru(2)	85.58(6)
Pt(1)–Pt(2)–Ru(4)	93.85(4)	Pt(3)–Ru(3)–Ru(1)	86.00(6)
Pt(3)–Pt(2)–Ru(1)	94.38(5)	Pt(2)–Ru(4)–Ru(6)	86.33(6)
Pt(3)–Pt(2)–Ru(5)	94.40(5)	Pt(3)–Ru(4)–Ru(5)	96.98(6)
Ru(1)–Pt(2)–Ru(4)	153.30(6)	Pt(1)–Ru(5)–Ru(4)	85.76(6)
Ru(1)–Pt(2)–Ru(5)	107.64(5)	Pt(2)–Ru(5)–Ru(6)	85.85(5)
Ru(2)–Pt(2)–Ru(4)	107.58(5)	Pt(1)–Ru(6)–Ru(4)	85.78(5)
Ru(2)–Pt(2)–Ru(5)	153.70(5)	Pt(3)–Ru(6)–Ru(5)	86.46(5)
Pt(1)–Pt(3)–Ru(2)	94.67(5)	Ru(4)–C(43)–O(43)	166(2)
Pt(1)–Pt(3)–Ru(4)	93.02(5)	Ru(6)–C(63)–O(63)	169(2)
Pt(2)–Pt(3)–Ru(3)	94.02(4)	M–C–O (av)	175(2)

(4)–Ru(5)–Ru(6) triangle, but the fourth hydride is a triply bridging ligand on the face of the Ru(1)–Ru(2)–Ru(3) triangle. The platinum–platinum distances (Pt(1)–Pt(2) = 2.629(1) Å, Pt(1)–Pt(3) = 2.635(1) Å, and Pt(2)–Pt(3) = 2.646(1) Å) are similar to those found in other layered mixed-metal clusters containing platinum triangles,[5a,b,6a–c] but the ruthenium–ruthenium distances (Ru(1)–Ru(2) = 3.084(2) Å, Ru(1)–Ru(3) = 3.043(2) Å, Ru(2)–Ru(3) = 3.054(3) Å, Ru(4)–Ru(5) = 3.002(2) Å, Ru(4)–Ru(6) = 3.024(2) Å, and Ru(5)–Ru(6) = 3.033(2) Å) are unusually long due to the presence of the bridging hydride ligands.[13] The compound $Pt_3Ru_6(CO)_{21}(\mu\text{-}CO)(\mu_3\text{-}H)_2$ (4) has a similar stacked arrangement of platinum and ruthenium triangles but has one more CO ligand (a bridge) and two fewer hydride ligands.[5a]

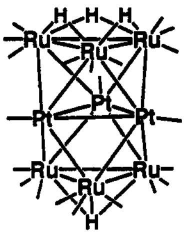

1

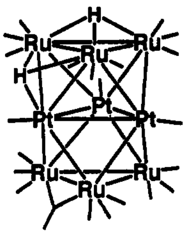

4

Due to a facile exchange process, the resonances of the hydride ligands are not observed at 25 °C in the ^1H NMR spectrum. However, this dynamical process was slowed down by reducing the temperature, and at −88 °C the individual resonances were clearly observed at δ −15.84 (3H) and −19.26 (1H) in the expected 3/1 intensity ratio. The ^{13}C NMR spectrum of 1 was obtained on a sample that was prepared from reagents containing 99% enriched ^{13}CO. At room temperature, the spectrum shows only a sharp singlet at 189.77 ppm. Apparently, all the CO ligands are dynamically averaged. At −85 °C the spectrum showed a sharp singlet at 189.7 ppm that appeared superimposed on a very broad hump that ranged from about 180 to 198 ppm. It is believed that the broad hump is due to resonance from a collection of CO ligands that are undergoing exchange that is neither resolved nor fully averaged on the NMR time scale. The sharp singlet is clearly due to CO ligands that are not being exchanged with the others. Since we could not obtain spectra at any lower temperatures, we cannot provide a detailed account of the dynamical motion that must be occurring among the CO ligands; however, at this temperature the hydride ligands are not being averaged (*vide supra*).

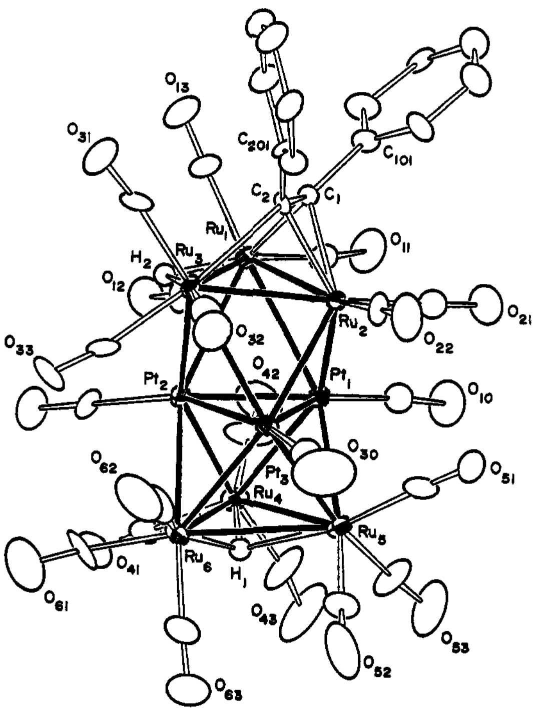

Figure 2. ORTEP diagram of $Pt_3Ru_6(CO)_{20}(\mu_3\text{-}PhC_2Ph)(\mu_3\text{-}H)(\mu\text{-}H)$ (2) showing 35% probability thermal ellipsoids for the non-hydrogen atoms.

The molecule contains 21 carbonyl ligands: each ruthenium atom has three carbonyl ligands, and each platinum atom has only one. There are a total of 124 valence electrons about the metal atoms, which is exactly the number predicted by the polyhedral skeletal electron pair theory for a cluster of nine transition-metal atoms having a face-shared bioctahedral structure.[14]

When treated with PhC_2Ph in a hexane solution at reflux, compound 1 was converted to the alkyne derivative $Pt_3Ru_6(CO)_{20}(\mu_3\text{-}PhC_2Ph)(\mu_3\text{-}H)(\mu\text{-}H)$ (2) in 25% yield. Small amounts of the known compounds $Ru_7Pt_3(CO)_{22}(\mu_3\text{-}H)_2$[2d] (7% yield) and $Pt_3Ru_6(CO)_{14}(\mu_3\text{-}PhC_2Ph)_3$[10] (5; 6% yield) were also formed in this reaction. The latter was derived from 2 by further reaction with PhC_2Ph. This was established independently by the reaction of 2 with PhC_2Ph, which produced 5 in 58% yield. Compound 2 was characterized by IR, ^1H and ^{13}C NMR, and a single-crystal X-ray diffraction analysis. An ORTEP diagram of its molecular structure is shown in Figure 2. Final atomic positional parameters for 2 are listed in Table 5. Selected bond distances and angles are given in Tables 6 and 7, respectively. This molecule contains a layered structure of Pt_3 and Ru_3 triangles that is similar to that of 1: Pt(1)–Pt(2) = 2.631(1) Å, Pt(1)–Pt(3) = 2.686(1) Å, Pt(2)–Pt(3) = 2.636(1) Å; Ru(1)–Ru(2) = 2.854(2) Å, Ru(1)–Ru(3) = 2.986(2) Å, Ru(2)–Ru(3) = 2.771(2) Å, Ru(4)–Ru(5) = 3.052(2) Å, Ru(4)–Ru(6) = 2.921(2) Å, Ru(5)–Ru(6) = 3.037(2) Å. Most interestingly, there is a triply bridging PhC_2Ph ligand that is coordinated to one of the ruthenium triangles, Ru(1)–Ru(2)–Ru(3). It exhibits the μ-$\|$ coordination mode that is commonly observed for triply

---

(13) Bau, R. *Struct. Bonding* **1981**, *44*, 1.

(14) Mingos, D. M. P.; May, A. S. In *The Chemistry of Metal Cluster Complexes*; Shriver, D. F., Kaesz, H. D., Adams, R. D., Eds.; VCH: New York, 1990; Chapter 2.

Table 5. Positional Parameters and *B*(eq) Values for $Pt_3Ru_6(CO)_{20}(\mu_3\text{-}PhC_2Ph)(\mu_3\text{-}H)(\mu\text{-}H)$ (2)

atom	*x*	*y*	*z*	*B*(eq), Å^2
Pt(1)	0.59576(08)	0.144718(14)	0.45921(04)	1.42(3)
Pt(2)	0.58280(08)	0.160622(15)	0.60633(04)	1.56(3)
Pt(3)	0.39850(08)	0.130536(14)	0.54598(04)	1.43(3)
Ru(1)	0.76887(14)	0.11581(03)	0.56866(08)	1.46(6)
Ru(2)	0.55650(14)	0.08771(02)	0.50489(08)	1.25(6)
Ru(3)	0.54900(15)	0.09906(03)	0.66329(08)	1.54(6)
Ru(4)	0.57741(16)	0.20345(03)	0.49374(09)	2.06(7)
Ru(5)	0.37340(16)	0.16612(03)	0.42168(09)	2.03(7)
Ru(6)	0.36105(16)	0.18908(03)	0.58767(09)	2.09(7)
O(10)	0.6941(18)	0.1475(04)	0.2986(08)	5(1)
O(11)	0.9079(17)	0.1202(04)	0.4127(08)	5(1)
O(12)	0.8975(15)	0.1723(03)	0.6200(09)	4.3(8)
O(13)	0.9724(19)	0.0887(04)	0.6665(08)	6(1)
O(20)	0.6722(19)	0.2036(03)	0.7304(09)	6(1)
O(21)	0.6150(16)	0.0793(03)	0.3347(08)	3.9(8)
O(22)	0.3402(15)	0.0480(03)	0.4788(09)	4.2(8)
O(30)	0.1542(17)	0.1017(04)	0.5238(13)	8(1)
O(31)	0.6424(16)	0.0647(03)	0.8027(08)	4.3(9)
O(32)	0.2948(17)	0.0727(03)	0.6792(09)	4.4(9)
O(33)	0.4609(19)	0.1456(03)	0.7814(08)	6(1)
O(41)	0.6065(15)	0.2543(03)	0.6042(09)	4.0(8)
O(42)	0.8441(19)	0.1992(03)	0.4575(11)	5(1)
O(43)	0.553(03)	0.2477(05)	0.3640(10)	10(2)
O(51)	0.3297(17)	0.1101(03)	0.3329(08)	4.4(9)
O(52)	0.103(02)	0.1776(07)	0.4187(14)	12(2)
O(53)	0.408(02)	0.2008(04)	0.2735(10)	9(1)
O(61)	0.3901(19)	0.2312(04)	0.7193(11)	7(1)
O(62)	0.2056(19)	0.1482(04)	0.6845(11)	6(1)
O(63)	0.1342(19)	0.2240(04)	0.5459(12)	7(1)
C(1)	0.7267(17)	0.0701(03)	0.5493(09)	1.3(3)
C(2)	0.6310(17)	0.0610(03)	0.5944(09)	1.2(7)
C(10)	0.662(02)	0.1459(04)	0.3598(12)	2.7(4)
C(11)	0.847(02)	0.1192(04)	0.4696(12)	3(1)
C(12)	0.8299(20)	0.1548(04)	0.6016(10)	2(1)
C(13)	0.895(02)	0.0988(04)	0.6315(12)	3(1)
C(20)	0.6390(20)	0.1876(04)	0.6830(11)	2(1)
C(21)	0.596(02)	0.0830(04)	0.3945(12)	2.7(4)
C(22)	0.422(02)	0.0623(04)	0.4910(11)	3(1)
C(30)	0.249(02)	0.1119(05)	0.5292(11)	3(1)
C(31)	0.617(02)	0.0771(04)	0.7484(12)	2(1)
C(32)	0.392(02)	0.0820(04)	0.6705(13)	3(1)
C(33)	0.495(02)	0.1316(05)	0.7326(12)	3(1)
C(41)	0.5938(19)	0.2355(04)	0.5642(12)	2(1)
C(42)	0.744(02)	0.1994(04)	0.4734(16)	4(1)
C(43)	0.562(03)	0.2294(05)	0.4075(14)	5(1)
C(51)	0.346(02)	0.1305(04)	0.3678(13)	3(1)
C(52)	0.203(03)	0.1737(07)	0.4195(17)	6(2)
C(53)	0.399(03)	0.1888(04)	0.3323(14)	5(1)
C(61)	0.388(02)	0.2153(05)	0.6695(14)	4(1)
C(62)	0.272(03)	0.1608(05)	0.6452(14)	4(1)
C(63)	0.220(03)	0.2110(04)	0.5637(14)	4(1)

bridging alkyne ligands at trimetallic centers.[15] The C(1)–C(2) distance in the PhC_2Ph ligand is 1.36(2) Å and is indicative of the presence of multiple-bond character. Complex 2 contains only two hydride ligands. One of these was found bridging the Ru(1)–Ru(3) edge of the Ru_3 triangle that contains the bridging PhC_2Ph ligand. The other is a triply bridging ligand spanning the face of the other triruthenium triangle. Note that the short Ru–Ru distances between the atoms Ru(1) and Ru(2) and between Ru(2) and Ru(3), where there are no bridging hydride ligands, are by far the shortest Ru–Ru distances in the molecule.

Two hydride ligands were lost in the transformation of 1 to 2. Evidence concerning the fate of the missing hydride ligands was obtained by performing the reaction of 1 with PhC_2Ph in benzene-d_6 solvent. An NMR spectrum of the reaction mixture showed a strong signal at 6.48 ppm that is attributed to (*Z*)-stilbene.[9] Accordingly, it is believed that the two hydride ligands that were lost from 1 in the formation of 2 were transferred to a second equivalent of PhC_2Ph to hydrogenate it to (*Z*)-stilbene.

Table 6. Intramolecular Distances (Å) for 2

Pt(1)–Pt(2)	2.632(1)	Ru(1)–C(12)	1.98(2)
Pt(1)–Pt(3)	2.687(1)	Ru(1)–C(13)	1.91(2)
Pt(1)–Ru(1)	2.965(2)	Ru(2)–Ru(3)	2.770(2)
Pt(1)–Ru(2)	2.744(1)	Ru(2)–C(1)	2.15(2)
Pt(1)–Ru(4)	2.745(1)	Ru(2)–C(2)	2.12(2)
Pt(1)–Ru(5)	2.681(2)	Ru(2)–C(21)	1.95(2)
Pt(1)–C(10)	1.85(2)	Ru(2)–C(22)	1.88(2)
Pt(2)–Pt(3)	2.636(1)	Ru(3)–C(2)	2.28(2)
Pt(2)–Ru(1)	2.942(2)	Ru(3)–C(31)	1.92(2)
Pt(2)–Ru(3)	2.990(2)	Ru(3)–C(32)	1.88(2)
Pt(2)–Ru(4)	2.746(2)	Ru(3)–C(33)	1.99(2)
Pt(2)–Ru(6)	2.752(2)	Ru(4)–Ru(5)	3.053(2)
Pt(2)–C(20)	1.90(2)	Ru(4)–Ru(6)	2.923(2)
Pt(3)–Ru(2)	2.690(2)	Ru(4)–C(41)	1.90(2)
Pt(3)–Ru(3)	2.963(2)	Ru(4)–C(42)	1.85(3)
Pt(3)–Ru(5)	2.693(2)	Ru(4)–C(43)	1.90(2)
Pt(3)–Ru(6)	2.789(1)	Ru(5)–Ru(6)	3.039(2)
Pt(3)–C(30)	1.85(3)	Ru(5)–C(51)	1.89(2)
Ru(1)–Ru(2)	2.854(2)	Ru(5)–C(52)	1.88(3)
Ru(1)–Ru(3)	2.986(2)	Ru(5)–C(53)	1.87(2)
Ru(1)–C(1)	2.16(1)	Ru(6)–C(61)	1.87(2)
Ru(1)–C(11)	1.91(2)	Ru(6)–C(62)	1.89(2)
		Ru(6)–C(63)	1.87(3)

Table 7. Intramolecular Bond Angles (deg) for 2

Pt(2)–Pt(1)–Ru(5)	94.75(4)	Pt(1)–Pt(3)–Ru(6)	91.66(4)
Pt(2)–Pt(1)–Ru(2)	88.70(4)	Pt(1)–Pt(3)–Ru(3)	93.10(5)
Ru(5)–Pt(1)–Ru(2)	105.81(5)	Ru(2)–Pt(3)–Ru(5)	106.99(5)
Ru(5)–Pt(1)–Ru(1)	152.11(5)	Ru(2)–Pt(3)–Ru(6)	148.48(5)
Pt(3)–Pt(1)–Ru(4)	93.23(4)	Ru(5)–Pt(3)–Ru(3)	152.31(5)
Pt(3)–Pt(1)–Ru(1)	92.67(4)	Ru(6)–Pt(3)–Ru(3)	111.58(5)
Ru(2)–Pt(1)–Ru(4)	147.96(5)	Ru(2)–Ru(1)–Pt(2)	80.84(5)
Ru(4)–Pt(1)–Ru(1)	109.94(5)	Pt(1)–Ru(1)–Ru(3)	87.25(6)
Pt(1)–Pt(2)–Ru(6)	93.69(4)	Pt(3)–Ru(2)–Ru(1)	95.13(5)
Pt(1)–Pt(2)–Ru(3)	93.61(4)	Pt(1)–Ru(2)–Ru(3)	96.26(5)
Pt(3)–Pt(2)–Ru(4)	94.34(4)	Ru(2)–Ru(3)–Pt(2)	81.37(4)
Pt(3)–Pt(2)–Ru(1)	94.26(4)	Pt(3)–Ru(3)–Ru(1)	86.96(5)
Ru(4)–Pt(2)–Ru(1)	110.60(5)	Pt(1)–Ru(4)–Ru(6)	87.68(5)
Ru(4)–Pt(2)–Ru(3)	153.22(5)	Pt(2)–Ru(4)–Ru(5)	84.59(5)
Ru(6)–Pt(2)–Ru(1)	154.28(5)	Pt(1)–Ru(5)–Ru(6)	86.51(5)
Ru(6)–Pt(2)–Ru(3)	111.83(5)	Pt(3)–Ru(5)–Ru(4)	86.56(5)
Pt(2)–Pt(3)–Ru(2)	89.76(5)	Pt(2)–Ru(6)–Ru(5)	84.77(5)
Pt(2)–Pt(3)–Ru(5)	94.36(4)	Pt(3)–Ru(6)–Ru(4)	87.42(5)
		M–C–O (av)	175(3)

As in 1, the hydride ligands in 2 are mobile on the NMR time scale and no hydride resonances were observed at 25 °C, but at −58 °C the resonances were clearly displayed (δ −17.97 (s, 1H), −18.71 (s, 1H)). The ^{13}C NMR spectrum of 2 was obtained at 25 °C in $CDCl_3$ solvent on a sample that was enriched to 99% with ^{13}CO. The spectrum exhibits seven resonances: δ 201.93 (s, 2CO), 197.02 (d, 2CO, $^3J_{^{13}C-^{13}C}$ = 11.1 Hz), 195.5 (s, 2CO), 194.69 (d, 1CO, $^3J_{^{13}C-^{13}C}$ = 11.1 Hz), 192.43 (s, 6CO), 190.34 (s, 4CO), 190.00 (s, 3CO). Interestingly, two of the resonances show splitting due to long-range ^{13}C–^{13}C coupling. Variable-temperature spectra were recorded in CD_2Cl_2 solvent, and the spectrum obtained at −85 °C is shown in Figure 3. This spectrum shows resonances at δ 202.3 (s, 2CO), 197.7 (d, 2CO, $^3J_{^{13}C-^{13}C}$ = 11 Hz), 195.9 (s, 2CO), 195.0 (d, 1CO, $^3J_{^{13}C-^{13}C}$ = 11 Hz), 192.3 (s, 6CO), 190.8 (s, 2CO), 190.4 (s, 2CO), and 190.1 (s, 3CO). Except for some minor shifts, most of the resonances correspond to those observed in the room-temperature spectrum obtained in $CDCl_3$ solvent. A significant difference is a splitting of the resonance at 190.34 into two resonances of equal intensity at 190.8 (2CO) and 190.4 (2CO) ppm. Interestingly, the separation of the 190.34 ppm resonance into two of equal intensity does not involve a collapse and re-formation of two new

---

(15) (a) Raithby, P. R.; Rosales, M. J. *Adv. Inorg. Chem. Radiochem.* **1985**, *29*, 169. (b) Sappa, E.; Tiripicchio, A.; Braunstein, P. *Chem. Rev.* **1983**, *83*, 203.

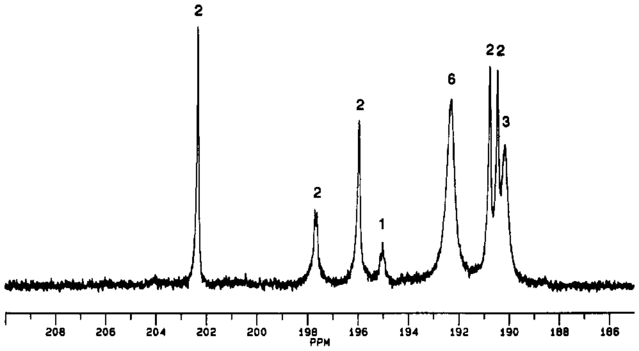

Figure 3. ^{13}C NMR spectrum of $Pt_3Ru_6(^{13}CO)_{20}(\mu_3\text{-}PhC_2Ph)(\mu_3\text{-}H)(\mu\text{-}H)$ (2*) recorded at −85 °C.

resonances but appears to be a simple temperature-dependent separation of two normal resonances as the temperature is lowered. We thus believe that this splitting is not due to a dynamic process. However, the resonances of intensity 6 (192.3 ppm) and 3 (190.1 ppm) have been broadened significantly at −85 °C. These broadenings are believed to be a result of true dynamical averaging processes that are still rapid but are just beginning to slow on the NMR time scale at this temperature. We were unable to record spectra at lower temperatures, and therefore, spectra in the slow-exchange region that would have shown the unaveraged resonances were not obtained.

To interpret the ^{13}C NMR spectrum, it must first be recognized that the molecule has reflection symmetry only, and only two CO ligands, C(20)–O(20) on Pt(2) and C(51)–O(51) on Ru(5), lie on this reflection plane. The spectrum at −85 °C can be easily interpreted by assuming that the alkyne ligand is not undergoing any dynamical motion relative to the cluster. The broad resonance at 190.1 ppm of intensity 3 is due to the three carbonyl ligands on Ru(5) that are being averaged by a tripodal rotation. Tripodal rotations of $M(CO)_3$ groupings are commonly observed in $M_3(CO)_9$ cluster complexes.[16] The broad resonance at 192.3 ppm of intensity 6 is due to tripodal rotations of the three carbonyl ligands on one of two possible pairs of equivalent metal atoms, either Ru(1) and Ru(3) or Ru(4) and Ru(6). Since there is a tripodal dynamical activity at Ru(5), it seems most likely that the other tripodal rotations are occurring at the Ru(4)–Ru(6) pair, because the ligand geometry of these metal atoms is more similar to that at Ru(5) than that of the Ru(1) and Ru(3) groups. Therefore, tripodal rotations are occuring rapidly at all three metal atoms on the Ru(4)–Ru(5)–Ru(6) triangle, and these are the only dynamical motions of the CO ligands in this molecule even at room temperature. The doublet at 197.7 ppm of intensity 2 and the singlet at 195.0 ppm of intensity 1 are assigned to the equivalent carbonyl ligands on Pt(1) and Pt(3) and the one on Pt(2), respectively. The observed shifts are consistent with those found for terminal CO ligands on Pt_3 triangles in the anions $[Pt_3(\mu\text{-}CO)_3(CO)_3]_n^{2-}$, ($n$ = 2–4), which lie in the range 196.7–203.7 ppm.[17] The presence of long-range coupling could be due to the fact that the carbonyl ligands lie approximately trans to one another. Finally, the four singlets of intensity 2 are assigned to the four pairs of CO ligands on the alkyne bridged ruthenium triangle, but specific assignments cannot be made at this time.

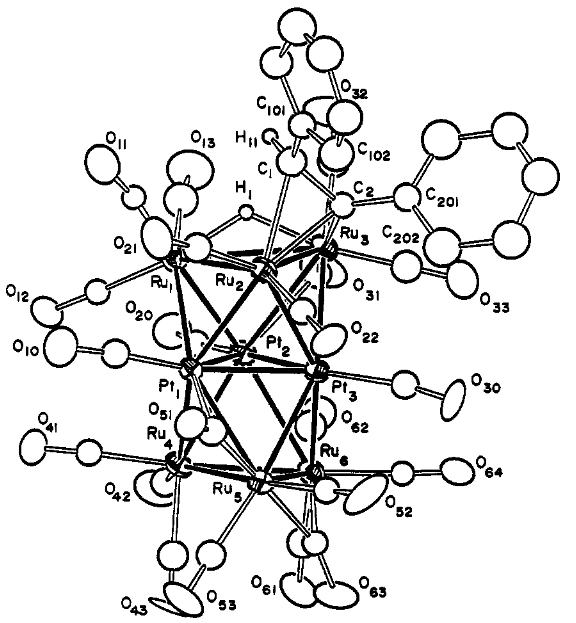

Figure 4. ORTEP diagram of $Pt_3Ru_6(CO)_{21}[\mu\text{-}PhCC(H)Ph](\mu\text{-}H)$ (3) showing 35% probability thermal ellipsoids for the non-hydrogen atoms.

Under an atmosphere of CO at 25 °C, compound **2** adds 1 equiv of CO to yield the new complex $Pt_3Ru_6(CO)_{21}[\mu\text{-}PhCC(H)Ph](\mu\text{-}H)$ (**3**), which can be isolated in 11% yield. $Ru_3(CO)_{12}$ and $Ru_4Pt_2(CO)_{18}$ are also formed due to degradation of the cluster. These products are also formed by the addition of CO to **3** (see below), and this may explain the relatively low yield of **3**. Compound **3** was characterized by IR, ^{1}H NMR, and a single-crystal X-ray diffraction analysis. An ORTEP diagram of the molecular structure of this complex is shown in Figure 4. Final atomic positional parameters for **3** are listed in Table 8. Selected bond distances and angles are given in Tables 9 and 10, respectively. This molecule also contains a layered structure of Pt_3 and Ru_3 triangles that is similar to that of **1** and **2**. The most interesting ligand is the diphenylvinyl ligand, PhCC(H)Ph, that bridges the Ru(2)–Ru(3) edge of the Ru(1)–Ru(2)–Ru(3) triangle. It exhibits the σ–π coordination mode that is commonly observed for these ligands.[18,19] The refined C(1)–C(2) distance is longer than those found for this ligand in similar bonding configurations in triruthenium clusters, 1.51(5) Å.[18] However, the estimated standard deviation is quite large, and this is probably due to the paucity of observed diffraction data. It is notable that the phenyl substituents have adopted a *cis* stereochemistry. The hydrogen atom on this ligand was not located crystallographically, but its identity was established unambiguously by its characteristic ^{1}H NMR shift, δ 5.26 ppm. The complex contains one hydride ligand, which was observed in the ^{1}H NMR spectrum at δ −22.77 ppm. This ligand was located and refined in the structural analysis. It is a bridging ligand that spans the Ru(1)–Ru(3) bond. As a result, the Ru(1)–Ru(3) bond is very long (3.131(5) Å), as expected for hydride-bridged metal–metal bonds.[13] Unlike **2**, the Ru(4)–Ru(5)–Ru(6)

---

[16] (a) Farrugia, L. J.; Rae, S. E. *Organometallics* **1992**, *11*, 196. (b) Farrugia, L. J. *J. Organomet. Chem.* **1990**, *394*, 515. (c) Farrugia, L. J. *Adv. Organomet. Chem.* **1990**, *31*, 301. (d) Rosenberg, E.; Thorsen, C. B.; Milone, L.; Aime, S. *Inorg. Chem.* **1985**, *24*, 231.

[17] Mingos, D. M. P.; Wardle, R. W. M. *Transition Met. Chem.* **1985**, *10*, 441.

[18] Deeming, A. J. *Adv. Organomet. Chem.* **1986**, *26*, 1.

[19] (a) Lugan, N.; Laurent, F.; Lavigne, G.; Newcomb, T. P.; Liimatta, E. W.; Bonnet, J.-J. *Organometallics* **1992**, *11*, 1351. (b) Cabeza, J. A.; Garcia-Granda, S.; Llamazares, A.; Riera, V.; Van der Maelen, J. F. *Organometallics* **1993**, *12*, 2973.

Table 8. Positional Parameters and B(eq) Values for $Pt_3Ru_6(CO)_{21}(\mu\text{-}CPhCHPh)(\mu\text{-}H)$ (3)

atom	x	y	z	B(eq), Å^2
Pt(1)	0.89560(14)	0.3409	0.73262(10)	3.13(7)
Pt(2)	0.79461(15)	0.14537(18)	0.65155(10)	3.47(7)
Pt(3)	0.67654(13)	0.3079	0.69745(09)	3.16(7)
Ru(1)	0.9464(03)	0.1263(03)	0.8021(02)	3.8(2)
Ru(2)	0.8042(03)	0.3019(03)	0.86169(18)	3.4(1)
Ru(3)	0.6899(03)	0.1046(03)	0.7902(02)	3.9(2)
Ru(4)	0.8791(03)	0.3084(03)	0.56108(19)	3.9(2)
Ru(5)	0.7497(03)	0.4909(03)	0.6205(02)	3.7(2)
Ru(6)	0.6454(03)	0.2927(03)	0.5249(02)	3.8(2)
O(10)	1.132(03)	0.403(03)	0.8163(19)	7(2)
O(11)	1.104(03)	0.156(03)	0.9742(18)	7(2)
O(12)	1.148(02)	0.123(03)	0.7294(17)	6(2)
O(13)	0.928(03)	−0.135(03)	0.810(02)	9(2)
O(20)	0.909(03)	−0.054(03)	0.595(02)	8(2)
O(21)	1.006(03)	0.419(03)	0.9810(17)	7(2)
O(22)	0.691(02)	0.533(03)	0.8595(18)	6(2)
O(30)	0.443(02)	0.402(04)	0.6831(20)	9(2)
O(31)	0.662(03)	−0.087(03)	0.6583(17)	7(2)
O(32)	0.704(04)	−0.109(03)	0.901(03)	12(3)
O(33)	0.441(03)	0.119(03)	0.7293(16)	7(2)
O(41)	1.137(02)	0.341(04)	0.6234(17)	9(2)
O(42)	0.891(03)	0.126(03)	0.428(02)	9(2)
O(43)	0.859(03)	0.494(03)	0.427(02)	8(2)
O(51)	0.900(02)	0.600(03)	0.7810(18)	6(1)
O(52)	0.584(03)	0.650(03)	0.6721(17)	9(2)
O(53)	0.857(03)	0.695(03)	0.548(02)	8(2)
O(61)	0.622(03)	0.306(04)	0.3385(17)	9(2)
O(62)	0.630(03)	0.034(03)	0.4874(17)	5(1)
O(63)	0.581(03)	0.535(03)	0.4492(15)	6(2)
O(64)	0.393(03)	0.285(03)	0.5045(16)	6(2)
C(1)	0.787(04)	0.196(04)	0.974(03)	5.1(9)
C(2)	0.684(03)	0.197(03)	0.900(02)	3.1(7)
C(10)	1.037(03)	0.379(03)	0.787(02)	4.0(8)
C(11)	1.037(03)	0.138(03)	0.909(02)	2.9(7)
C(12)	1.067(03)	0.116(03)	0.752(02)	3.5(8)
C(13)	0.943(04)	−0.038(05)	0.813(03)	6(1)
C(20)	0.870(04)	0.025(04)	0.611(02)	4.0(8)
C(21)	0.931(03)	0.369(04)	0.939(02)	4.1(8)
C(22)	0.738(03)	0.439(03)	0.861(02)	3.5(8)
C(30)	0.528(03)	0.359(03)	0.692(02)	3.9(8)
C(31)	0.681(04)	−0.003(04)	0.695(03)	4.3(8)
C(32)	0.692(04)	−0.030(05)	0.859(03)	6(1)
C(33)	0.539(04)	0.104(04)	0.751(03)	5(1)
C(41)	1.038(03)	0.330(04)	0.603(02)	4.0(8)
C(42)	0.887(04)	0.197(04)	0.475(03)	4.6(9)
C(43)	0.867(04)	0.433(04)	0.478(03)	6(1)
C(51)	0.856(03)	0.530(04)	0.730(03)	4.0(8)
C(52)	0.645(03)	0.589(03)	0.651(02)	3.7(8)
C(53)	0.819(04)	0.621(04)	0.576(03)	5(1)
C(61)	0.632(03)	0.294(04)	0.411(03)	5.4(9)
C(62)	0.646(04)	0.128(04)	0.513(03)	5.0(9)
C(63)	0.632(03)	0.485(03)	0.509(03)	3.1(7)
C(64)	0.488(03)	0.292(03)	0.512(02)	2.8(7)
H(1)	0.84(03)	0.10(03)	0.869(19)	5.0

Table 9. Intramolecular Distances (Å) for 3

Pt(1)–Pt(2)	2.742(2)	Ru(1)–Ru(3)	3.131(5)
Pt(1)–Pt(3)	2.634(3)	Ru(1)–H(1)	2.0(3)
Pt(1)–Ru(1)	2.728(4)	Ru(2)–Ru(3)	2.765(6)
Pt(1)–Ru(2)	2.726(4)	Ru(2)–C(1)	2.30(4)
Pt(1)–Ru(4)	2.828(4)	Ru(2)–C(2)	2.15(4)
Pt(1)–Ru(5)	2.801(4)	Ru(3)–C(2)	2.13(4)
Pt(1)–C(51)	2.24(4)	Ru(3)–C(31)	1.99(4)
Pt(2)–Pt(3)	2.614(2)	Ru(3)–H(1)	1.9(3)
Pt(2)–Ru(1)	2.688(4)	Ru(4)–Ru(5)	2.972(5)
Pt(2)–Ru(3)	2.977(4)	Ru(4)–Ru(6)	2.789(5)
Pt(2)–Ru(4)	2.784(4)	Ru(5)–Ru(6)	2.876(5)
Pt(2)–Ru(6)	2.926(4)	Ru(5)–C(51)	1.98(4)
Pt(2)–C(31)	2.44(4)	Ru(5)–C(63)	2.01(4)
Pt(3)–Ru(2)	2.750(4)	Ru(6)–C(63)	2.23(4)
Pt(3)–Ru(3)	2.783(4)	C(1)–C(2)	1.51(5)
Pt(3)–Ru(5)	2.746(4)	Pt–C (av)	1.86(4)
Pt(3)–Ru(6)	2.793(4)	Ru–C (av)	1.89(5)
Ru(1)–Ru(2)	3.022(5)	O–C (av)	1.15(4)
		Pt(2)–C(62)	2.52(4)

Table 10. Intramolecular Bond Angles (deg) for 3

Pt(2)–Pt(1)–Ru(2)	91.1(1)	Pt(1)–Ru(1)–Ru(3)	86.3(1)
Pt(2)–Pt(1)–Ru(5)	93.3(1)	Pt(2)–Ru(1)–Ru(2)	86.1(1)
Pt(3)–Pt(1)–Ru(1)	93.70(8)	Pt(1)–Ru(2)–Ru(3)	94.1(1)
Pt(3)–Pt(1)–Ru(4)	88.6(1)	Pt(3)–Ru(2)–Ru(1)	85.2(1)
Ru(1)–Pt(1)–Ru(4)	104.5(1)	Pt(2)–Ru(3)–Ru(2)	85.6(1)
Ru(1)–Pt(1)–Ru(5)	150.6(1)	Pt(3)–Ru(3)–Ru(1)	82.6(1)
Ru(2)–Pt(1)–Ru(4)	147.4(1)	Pt(1)–Ru(4)–Ru(6)	90.4(1)
Ru(2)–Pt(1)–Ru(5)	107.1(1)	Pt(1)–Ru(5)–Ru(6)	89.2(1)
Pt(1)–Pt(2)–Ru(3)	89.2(1)	Pt(3)–Ru(5)–Ru(4)	83.6(1)
Pt(1)–Pt(2)–Ru(6)	89.3(1)	Pt(2)–Ru(6)–Ru(5)	88.1(1)
Pt(3)–Pt(2)–Ru(1)	95.1(1)	Pt(3)–Ru(6)–Ru(4)	86.3(1)
Pt(3)–Pt(2)–Ru(4)	89.9(1)	Ru(2)–C(1)–C(101)	121(3)
Ru(1)–Pt(2)–Ru(4)	106.8(1)	C(2)–C(1)–C(101)	122(3)
Ru(1)–Pt(2)–Ru(6)	148.8(1)	Ru(3)–C(2)–C(1)	118(3)
Ru(3)–Pt(2)–Ru(4)	146.5(1)	Ru(3)–C(2)–C(201)	125(3)
Ru(3)–Pt(2)–Ru(6)	109.0(1)	C(1)–C(2)–C(201)	114(3)
Pt(1)–Pt(3)–Ru(3)	95.7(1)	Pt(2)–C(31)–O(31)	120(3)
Pt(1)–Pt(3)–Ru(6)	94.5(1)	Ru(3)–C(31)–O(31)	156(4)
Pt(2)–Pt(3)–Ru(2)	93.4(1)	Pt(1)–C(51)–O(51)	126(3)
Pt(2)–Pt(3)–Ru(5)	97.5(1)	Ru(5)–C(51)–O(51)	150(3)
Ru(2)–Pt(3)–Ru(5)	108.0(1)	Ru(5)–C(63)–O(63)	147(3)
Ru(2)–Pt(3)–Ru(6)	153.7(1)	Ru(6)–C(63)–O(63)	127(3)
Ru(3)–Pt(3)–Ru(5)	158.0(1)	Ru–C–O (av)	173(5)
Ru(3)–Pt(3)–Ru(6)	119.1(1)		

triangle has 10 CO ligands instead of 9. One of these is a bridging ligand across the Ru(5)–Ru(6) bond, C(63)–O(63). Two others are semibridging ligands to two of the platinum atoms. One of these is a fairly strong semibridge Pt(1)···C(51) = 2.24(4) Å), while the other is a relatively weak one (Pt(2)···C(62) = 2.52(4) Å.

When 3 was treated with CO (1 atm) at room temperature for 2 days and then heated to reflux for 3 h under CO, (*Z*)-stilbene was formed in 85% yield by the transfer of the hydride ligand to the diphenylvinyl ligand and its elimination from the complex. The cluster was itself degraded, but much of the metal content was recovered in the form of the two known cluster complexes $Ru_3(CO)_{12}$ and $Pt_2Ru_4(CO)_{18}$.

Discussion

We have observed previously that the reaction of $Pt_2Os_4(CO)_{18}$ with H_2 yields hydride-rich platinum–osmium cluster complexes having structures based on vertex-shared triangles and tetrahedra.[20] The reaction of $Pt_2Ru_4(CO)_{18}$ with H_2 has yielded no complexes analogous to those of platinum–osmium complexes. Instead, the nine-metal cluster 1 that possesses layer-segregated stacks of platinum and ruthenium triangles was formed. Similarly, stacked platinum–osmium cluster complexes have been prepared, but these were obtained by different procedures.[3a–c] Studies of certain large nickel–platinum cluster complexes have shown that the platinum will segregate from the nickel to form Pt_3 triangles[21] and Pt_6 octahedra[22] in the center of the overall cluster grouping.

A summary of the results of this study are shown in Scheme 1. By decarbonylation at 97 °C in the presence of hydrogen, the new nine-metal cluster complex 1 was formed in a good yield; it has the same relative platinum/ruthenium composition as the starting material $Pt_2Ru_4(CO)_{18}$. We believe that this has occurred by an aggregation process that involves trinuclear $PtRu_2$ fragments. Our studies of the reaction of $Pt_2Ru_4(CO)_{18}$ with diphenyl-

---

(20) Adams, R. D.; Pompeo, M. P.; Wu, W. *Inorg. Chem.* **1991**, *32*, 2425.

(21) (a) Ceriotti, A.; Demartin, F.; Longoni, G.; Manassero, M.; Piva, G; Piro, G.; Sansoni, M.; Heaton, B. T. *J. Organomet. Chem. 1986*, 301, *C5*.

(22) Ceriotti, A.; Demartin, F.; Longoni, G.; Manassero, M.; Marchionna, M.; Piva, G.; Sansoni, M. *Angew. Chem., Int. Ed. Engl.* **1985**, *24*, 697.

Scheme 1

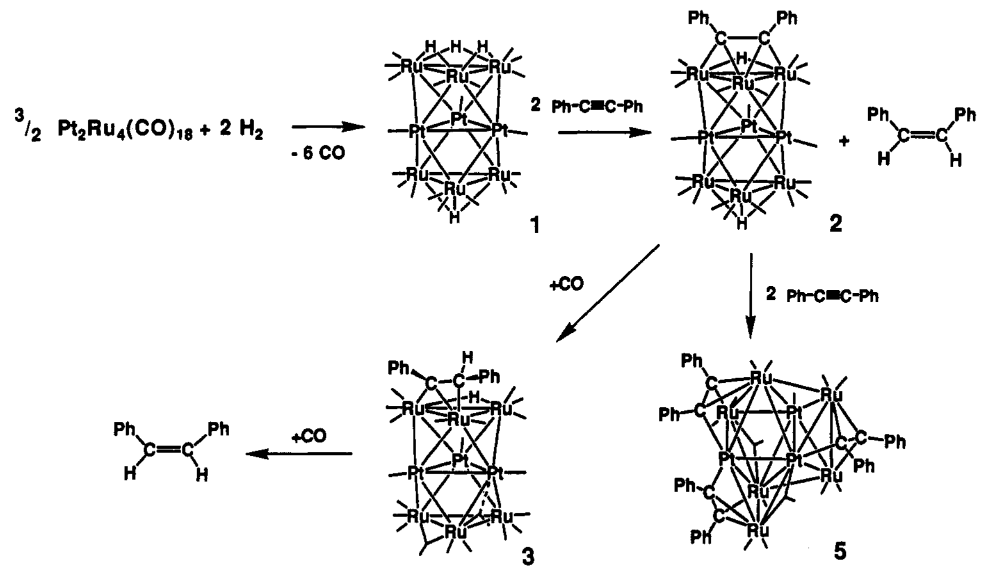

acetylene have shown similar aggregation processes and also produced evidence for fragmentation to trinuclear $PtRu_2$ fragments.[14] It has also been shown that the structurally similar complex $Pt_2Os_4(CO)_{18}$ can be split by CO to yield the mixed-metal trinuclear complex $PtOs_2(CO)_{10}$.[23] The structure of compound 1 exhibits a layer-segregated arrangement of the two types of metals. This arrangement has been observed recently for a number of mixed-metal clusters containing three or more platinum atoms[5a,b,6a–c] and has been observed at least once for a nonplatinum-containing cluster.[24]

The reaction of 1 with PhC_2Ph yields the PhC_2Ph complex 2, in which the PhC_2Ph ligand is coordinated to one of the triruthenium triangles. Two hydride ligands were lost from the cluster in this reaction. The accompanying formation of (*Z*)-stilbene seems to explain their fate fully. We believe that the preference of the PhC_2Ph ligand for coordination to the ruthenium triangles is important for its subsequent transformations. In our previous studies of the layer-segregated cluster complex $Pt_4Os_6(CO)_{22}(COD)$ we observed that COD is added selectively to the platinum triangle upon photodecarbonylation of the complex.[6a] Such coordination preferences[3a,25] could be important in catalysis by mixed-metal complexes or metal alloys[26] when two different reagents are involved in the reaction.

Compound 2 reacts with CO through a process that induces the transfer of both hydride ligands to the PhC_2Ph ligand to yield (*Z*)-stilbene. Fortunately, we were able to isolate and structurally characterize small amounts of the compound 3 formed by the addition of 1 equiv of CO to 2. It is, indeed, an intermediate in the (*Z*)-stilbene-forming process, and its structure provides valuable details with respect to the mechanism. The number of CO ligands on the ruthenium triangle that does not contain the PhC_2Ph ligand was increased by 1 to give a total of 10. The triply bridging hydride ligand that occupied the face of that Ru_3 triangle was shifted to the other end of the molecule, and one of the hydride ligands was transferred to the PhC_2Ph ligand. The PhC_2Ph ligand was transformed to a diphenylvinyl ligand, and it was shifted to an edge of the Ru_3 triangle. It has adopted the σ–π coordination mode that is typical of such ligands, and it serves as a three-electron donor. Thus, the formation of the C–H bond results in the removal of two electrons from the valence shell of the cluster, and this counterbalances the addition of the two electrons to the cluster by the CO addition. Most importantly, the phenyl groups have adopted the *cis* configuration which is a prerequisite to the formation of the (*Z*)-stilbene in the final step. Compound 3 reacts with CO to yield (*Z*)-stilbene, but the loss of the (*Z*)-stilbene and accompanying CO addition results in a species that is unstable and the cluster is degraded to $Ru_3(CO)_{12}$ and $Pt_2Ru_4(CO)_{18}$.

In the presence of hydrogen and free diphenylacetylene the formation of (*Z*)-stilbene from 2 occurs even in the absence of CO and this process repeats itself catalytically.[7] The catalytic activity is unusually high for a cluster complex and is also highly selective for the formation of (*Z*)-stilbene (eq 1). A full report of our studies of this

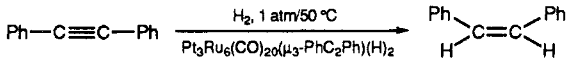

catalytic activity of 2 is being prepared.

Acknowledgment. These studies were supported by the National Science Foundation under Grant No. CHE-9224141. We thank Dr. Paul Swepston of The Molecular Structure Corp. for assistance with the structural analysis of compound 2.

Supplementary Material Available: Tables of hydrogen atom positional parameters and anisotropic thermal parameters for 1–3 (14 pages). Ordering information is given on any current masthead page.

OM9401162

---

(23) Sundberg, P. *J. Chem. Soc., Chem. Commun.* **1987**, 1307.

(24) Della Pergola, R.; Garlaschelli, L.; Demartin, F.; Manassero, M.; Masciocchi, N.; Longoni, G. *J. Chem. Soc., Dalton Trans.* **1988**, 201.

(25) (a) Matsuzaka, H.; Kodama, T.; Uchida, Y.; Hidai, M. *Organometallics* **1988**, *7*, 1608. (b) Hidai, M.; Matsuzaka, H. *Polyhedron* **1988**, *7*, 2369. (c) Rossi, S.; Pursiainen, J.; Pakkanen, T. A. *J. Organomet. Chem.* **1990**, *397*, 81. (d) Braunstein, P.; Mourey, L.; Rosé, J.; Granger, P.; Richert, T.; Balegroune, F.; Grandjean, D. *Organometallics* **1992**, *11*, 2628.

(26) Goodman, D. W.; Houston, J. E. *Science* **1987**, *236*, 403.